

Wilms tumor reveals DNA repair gene hyperexpression is linked to lack of tumor immune infiltration

Emily F Higgs ¹, Riyue Bao ^{2,3}, Ken Hatogai,¹ Thomas F Gajewski¹

To cite: Higgs EF, Bao R, Hatogai K, *et al.* Wilms tumor reveals DNA repair gene hyperexpression is linked to lack of tumor immune infiltration. *Journal for ImmunoTherapy of Cancer* 2022;**10**:e004797. doi:10.1136/jitc-2022-004797

► Additional supplemental material is published online only. To view, please visit the journal online (<http://dx.doi.org/10.1136/jitc-2022-004797>).

Accepted 29 April 2022



© Author(s) (or their employer(s)) 2022. Re-use permitted under CC BY-NC. No commercial re-use. See rights and permissions. Published by BMJ.

¹Pathology, University of Chicago Department of Medicine, Chicago, Illinois, USA

²Medicine, University of Pittsburgh Medical Center, Pittsburgh, Pennsylvania, USA

³UPMC Hillman Cancer Center, Pittsburgh, Pennsylvania, USA

Correspondence to

Dr Thomas F Gajewski;
tgajewsk@medicine.bsd.
uchicago.edu

ABSTRACT

Background A T cell-rich tumor microenvironment has been associated with improved clinical outcome and response to immune checkpoint blockade therapies in several adult cancers. Understanding the mechanisms for lack of immune cell infiltration in tumors is critical for expanding immunotherapy efficacy. To gain new insights into the mechanisms of poor tumor immunogenicity, we turned to pediatric cancers, which are generally unresponsive to checkpoint blockade.

Methods RNA sequencing and clinical data were obtained for Wilms tumor, rhabdoid tumor, osteosarcoma, and neuroblastoma from the Therapeutically Applicable Research to Generate Effective Treatments (TARGET) database, and adult cancers from The Cancer Genome Atlas (TCGA). Using an 18-gene tumor inflammation signature (TIS) representing activated CD8⁺ T cells, we identified genes inversely correlated with the signature. Based on these results, adult tumors were also analyzed, and immunofluorescence was performed on metastatic melanoma samples to assess the MSH2 relationship to anti-programmed cell death protein-1 (PD-1) efficacy.

Results Among the four pediatric cancers, we observed the lowest TIS scores in Wilms tumor. TIS scores were lower in Wilms tumors compared with matched normal kidney tissues, arguing for loss of endogenous T cell infiltration. Pathway analysis of genes upregulated in Wilms tumor and anti-correlated with TIS revealed activated pathways involved DNA repair. The majority of adult tumors in TCGA also showed high DNA repair scores associated with low TIS. Melanoma samples from an independent cohort revealed an inverse correlation between MSH2⁺ tumor cells and CD8⁺ T cells. Additionally, melanomas with high MSH2⁺ tumor cell numbers were largely non-responders to anti-PD-1 therapy.

Conclusions Increased tumor expression of DNA repair genes is associated with a less robust immune response in Wilms tumor and the majority of TCGA tumor types. Surprisingly, the negative relationship between DNA repair score and TIS remained strong across TCGA when correcting for mutation count, indicating a potential role for DNA repair genes outside of preventing the accumulation of mutations. While loss of DNA repair machinery has been associated with carcinogenesis and mutational antigen generation, our results suggest that hyperexpression of DNA repair genes might be prohibitive for antitumor immunity, arguing for pharmacologic targeting of DNA repair as a potential therapeutic strategy.

Key messages

- ⇒ This study focused on the relatively non-T cell-inflamed Wilms tumor and identified differentially expressed genes in Wilms tumors compared with other pediatric tumor types, adult kidney tumor types, and genes that anti-correlated with T-cell inflammation signature within Wilms tumors.
- ⇒ Pathway analysis of these genes revealed high expression of DNA repair factors in non-T cell-inflamed Wilms tumors.
- ⇒ This observation was also seen across many of the adult tumors in TCGA (The Cancer Genome Atlas), and in metastatic melanoma samples stained for CD8, MSH2, and SOX10, there was a negative association between CD8⁺ (T cell) numbers and MSH2⁺ SOX10⁺ (MSH2-expressing tumor cell) numbers.
- ⇒ This suggests that high levels of the DNA repair protein MSH2 are anti-correlated with T cells in these samples, and we also found that patients with high MSH2⁺ SOX10⁺ tumor cell counts tended to be non-responders to anti-programmed cell death protein-1 therapy.
- ⇒ Loss of DNA repair factors has been associated with increased tumor immunogenicity, but to our knowledge this is the first implication of high DNA repair levels with the non-T cell-inflamed phenotype.

BACKGROUND

Wilms tumor is the most common pediatric kidney malignancy and affects approximately 1 in 10,000 children.¹ While the characterization of endogenous immune responses to adult tumors has led to the development of successful immunotherapeutic strategies, knowledge of pediatric antitumor immunity remains limited. Compared with adult tumors, pediatric tumors tend to have sparse neoantigens as well as an increased degree of stemness, which have been associated with resistance to immune-mediated elimination.² Wilms tumors in particular have a limited number of genetic aberrations and patients demonstrate a reduced autoantibody responses compared with patients with neuroblastoma, which indicates that fewer

immunogenic antigens are present.³ In the three major adult kidney cancer types, tumor inflammation signature (TIS) scores predict response to checkpoint blockade immunotherapy, while tumor mutational burden (TMB) does not.⁴ Renal clear cell carcinoma (KIRC) has the second highest TIS among all The Cancer Genome Atlas (TCGA) adult tumor types and is relatively responsive to immunotherapy without having a particularly high mutation load.⁵ On the other hand, chromophobe renal cell carcinoma (KICH) and kidney renal papillary cell carcinoma (KIRP) have similar mutation loads to KIRC, but lower TIS scores and demonstrate early evidence of low responsiveness to programmed cell death protein-1 (PD-1) blockade.⁶

The most commonly mutated gene in Wilms tumor is *CTNBI*, and other recurring mutations also promote Wnt pathway activation.⁷ Interestingly, active β -catenin signaling associates with immune exclusion across adult tumors and mechanistically promotes T cell exclusion in mouse melanoma models.^{8,9} Due to these and other factors, one might expect Wilms tumors to be relatively non-inflamed. While some studies with limited numbers of patients have reported on the presence of T and natural killer cells in Wilms tumors,¹⁰ others have observed low programmed death-ligand 1 (PD-L1) expression, which may indicate sparse T cell infiltration.¹¹ Additionally, Wilms tumors with lower CD8⁺ TIL scores are associated with larger size, increased invasiveness and metastasis, and shorter overall patient survival.¹² These results suggest that when T cell inflammation does occur in Wilms tumors, it can be associated with improved prognosis. A deeper characterization of pediatric tumors, especially those with low TMB and low T cell inflammation, may shed light on tumor-intrinsic mechanisms of immune evasion relevant to adult tumors as well.

METHODS

RNA sequencing and TIS

RNA sequencing data were downloaded from the Genomic Data Commons (Data Release 13.0) for TCGA samples and the Therapeutically Applicable Research to Generate Effective Treatments (TARGET) database for pediatric samples. Raw read counts were processed by trimmed mean of M values normalization followed by \log_2 transformation. TIS were calculated as the median of normalized \log_2 -expression of the following 18 genes: *PSMB10*, *HLA-DQA1*, *HLA-DRB1*, *CMKLR1*, *HLA-E*, *NKG7*, *CD8A*, *CCL5*, *CXCL9*, *CD27*, *CXCR6*, *IDO1*, *STAT1*, *TIGIT*, *LAG3*, *CD274*, *PDCD1LG2*, and *CD276*. CD8⁺ T cell percentages from single-cell RNA sequencing data¹³ were calculated as the percentage of cells in CD8-specific clusters (*IN10*, *IT2*, *IT3*, *IT18*) per total cells in each sample that passed quality control (excluding those classified as indistinct).

Correlation between gene signatures and adjustment for TMB

Correlations were performed between TIS and DNA repair gene signatures in each tumor type. TCGA TMB

data from whole exome sequencing analyzed with MutSig V.2.0 were downloaded from <https://gdac.broadinstitute.org/>, and TMB was taken as the total number of mutations in each tumor sample. One patient with outlier melanoma with 24,930 mutations was excluded from analysis. To remove the effects of TMB from the analysis of DNA repair score and TIS, the following linear regression models were fit: DNA repair score $\sim\log_2$ (TMB) and TIS $\sim\log_2$ (TMB). The residuals between these two models were correlated to adjust for the TMB effect.

Patient samples

Immunofluorescence staining was performed on pretreatment tumor samples from a cohort of 26 patients with metastatic melanoma treated with anti-PD-1 therapy (either nivolumab or pembrolizumab). The study Protocol was reviewed and approved by the institutional review board at the University of Chicago. We conducted the study in accordance with the Protocol with subsequent amendments and with the Declaration of Helsinki. All patients provided written informed consent for use of their samples and clinical data.

Multiplex immunohistochemistry

Sections of 5 μ m from formalin-fixed paraffin embedded blocks were stained using Opal multiplex kit (AKOYA Bioscience). Primary antibodies for MSH2 (D24B5, 1:200), CD8 (M7103, 1:200), and SOX10 (20B7, 1:200) were used. Slides were counterstained with DAPI and mounted before imaging with the Vectra Polaris Imaging System (AKOYA Bioscience) at 20 \times resolution. On each image, five tumor regions of interest (ROI) that had the most abundant CD8⁺ cell infiltration were selected. ROIs were analyzed using inForm Cell Analysis software 2.4.6781.17769 (AKOYA Bioscience). Tissue segmentation, cell segmentation, and cell phenotyping were performed using a random forest machine learning approach. Cell phenotypes were determined by building a training set of manually annotated positive and negative cells for SOX10, CD8, and MSH2. Trained classifiers were expanded for all images using batch analysis. The numbers of each cell phenotype were calculated as the total number in tumor areas of each 20 \times ROI.

Statistical analysis

Statistical analyses were performed using GraphPad Prism (GraphPad) V.9.0.0 with the exception of RNA sequencing data which was performed in R V.4.0.2 using RStudio. Significance unless described otherwise was determined by Student's t-test and expressed as p values, shown as asterisks (*, $p < 0.05$; **, $p < 0.01$; ***, $p < 0.001$; ****, $p < 0.0001$).

RESULTS

We first aimed to characterize the T-cell inflammation status of Wilms tumor samples in the TARGET database using gene expression profiling. To do so, we calculated

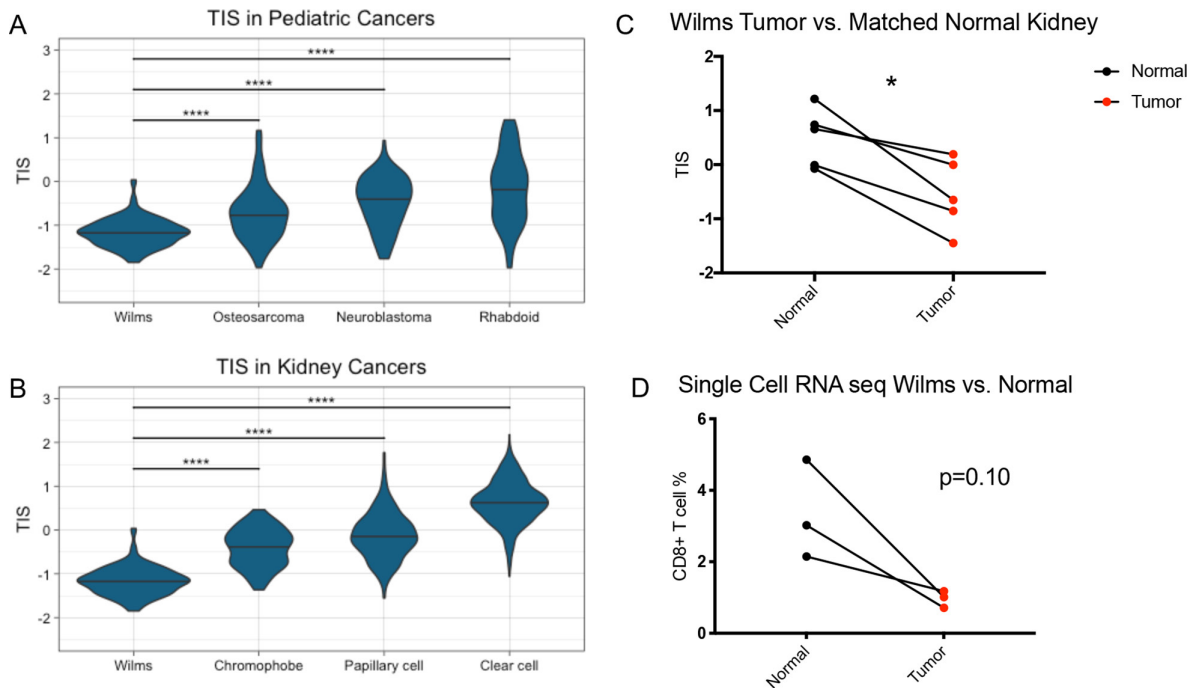


Figure 1 Wilms tumors have lower TIS than other pediatric cancer types, adult kidney cancer types, and matched normal kidney samples. (A) TIS scores in Wilms tumor and the other pediatric tumor types osteosarcoma, neuroblastoma, and rhabdoid tumor. (B) TIS scores in Wilms tumors and the other adult kidney tumor types chromophobe, papillary cell, and clear cell renal carcinoma. Two-way analysis of variance test. ****, $p < 0.0001$. (C) TIS scores in Wilms tumor versus matched normal kidney samples. (D) Percentage of CD8⁺ T cells in Wilms tumor samples by single-cell RNA sequencing versus matched normal tissue. Two-sided paired t-test. *, $p < 0.05$. seq, sequencing; TIS, tumor inflammation signature

the TIS score for each Wilms tumor sample using a previously defined 18-gene signature designed to measure adaptive antitumor immune responses.⁴ We then compared TIS scores from 120 Wilms tumor samples to 149 neuroblastoma samples, 84 osteosarcoma samples, and 65 rhabdoid tumor samples present in the TARGET database. Compared with the other pediatric cancer types tested, Wilms tumor samples had significantly lower TIS scores ($p < 0.0001$) (figure 1A), suggesting reduced endogenous antitumor immune responses. We also examined Wilms TIS in relation to adult kidney tumors from TCGA, including 538 KIRC samples, 288 KIRP samples, and 65 KICH samples. Among the adult kidney tumor types, KIRC had the highest TIS scores, while KICH had the lowest (figure 1B), which has been previously reported.¹⁴ However, Wilms tumor samples demonstrated significantly lower TIS scores than any of the adult tumor samples including KICH ($p < 0.0001$), which is one of the least inflamed tumor types across adult tumors.

To evaluate whether this was a characteristic of pediatric kidneys being non-T cell-inflamed rather than a feature of Wilms tumors, we analyzed the four patients in the TARGET database with paired RNA sequencing for Wilms tumor and adjacent normal kidney tissue. In these patients, the Wilms tumor samples had significantly lower TIS scores than matched normal samples ($p = 0.013$) (figure 1C). Additionally, in a published single-cell RNA sequencing data set,¹³ Wilms tumors demonstrated reduced CD8⁺ T cell percentages when compared with

paired normal kidney samples ($p = 0.10$) (figure 1D). Taken together, Wilms tumors exhibited lower TIS scores than other pediatric tumor types, other adult kidney tumor types, and matched normal samples, as well as having fewer CD8⁺ T cells by single-cell RNA sequencing.

To better understand the non-T cell-inflamed Wilms tumor phenotype by gene expression profiling, we used three separate approaches to identify genes that are both upregulated in Wilms tumor and anti-correlated with TIS. We first identified genes that were differentially expressed and upregulated in Wilms tumor compared with adult kidney cancers. Next, we identified the genes most significantly upregulated in Wilms tumor compared with matched normal tissue. We then determined which genes were most strongly anti-correlated with TIS scores in Wilms tumor samples (online supplemental file 1A). The intersection of these three methods identified 496 genes that met our criteria of being over-expressed in Wilms tumor and negatively associated with T cell inflammation (online supplemental table 1). The top pathways for these genes revealed by Ingenuity Pathway Analysis included several related to DNA damage, cell cycle checkpoint, and DNA repair (online supplemental figure 1B). The candidate genes were not limited to one type of DNA repair and instead represented multiple pathways including mismatch repair, nucleotide excision repair, and homologous recombination (online supplemental table 2). This suggests that genes related to the DNA damage response are

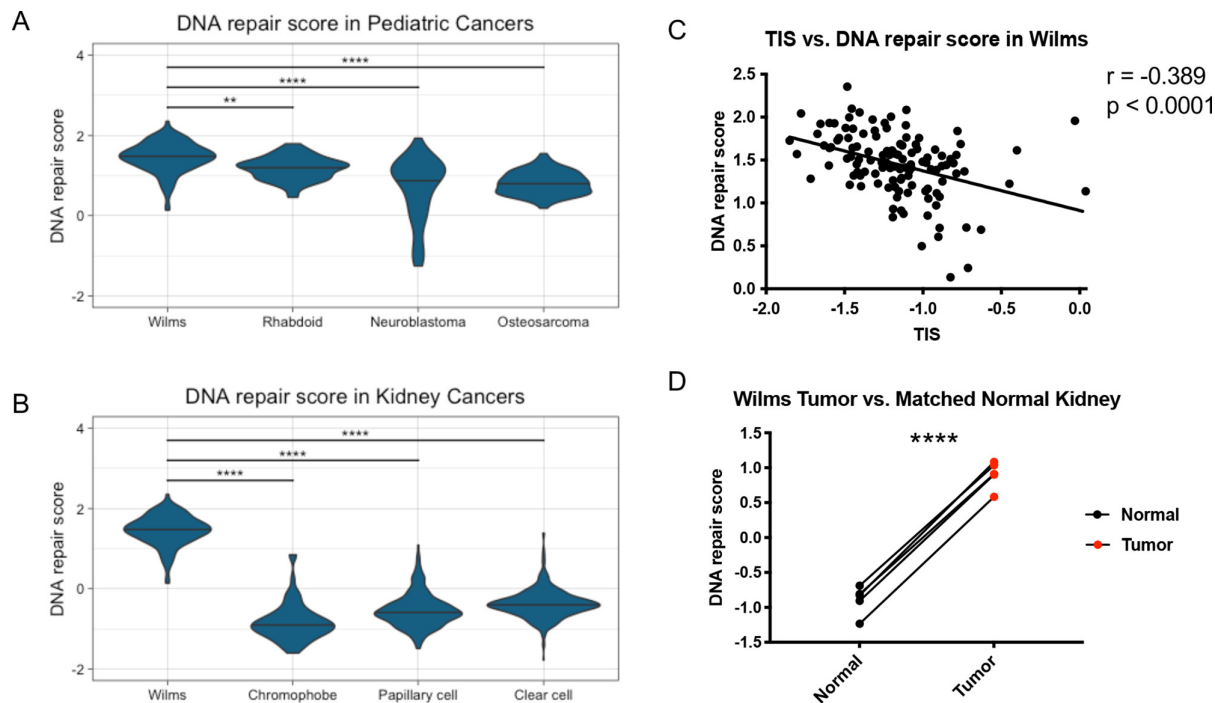


Figure 2 Wilms tumors have higher DNA repair scores than other pediatric cancer types, adult kidney cancer types, and matched normal kidney samples. (A) DNA repair scores in Wilms tumor and the other pediatric tumor types osteosarcoma, neuroblastoma, and rhabdoid tumor. (B) DNA repair scores in Wilms tumor and the other adult kidney tumor types chromophobe, papillary cell, and clear cell renal carcinoma. Two-way analysis of variance test. **, $p < 0.01$; ****, $p < 0.0001$. (C) Correlation between TIS and DNA repair score in Wilms tumor samples. Pearson's correlation $r = -0.389$, $p < 0.0001$. (D) DNA repair scores in Wilms tumor versus matched normal kidney samples. Two-sided paired t-test. ****, $p < 0.0001$. TIS, tumor inflammation signature

upregulated and associated with the non-T cell-inflamed phenotype in Wilms tumor.

To test this hypothesis, we curated a list of DNA repair genes by filtering the 496 genes previously identified by the 480 genes present in the MSigDB GO DNA Repair gene signature (online supplemental file 2, online supplemental table 3). This resulted in a list of 50 genes that were related to DNA repair, upregulated in Wilms tumor, and anti-correlated with TIS in Wilms tumor (online supplemental table 4). This 50-gene DNA repair signature was then used to calculate DNA repair expression scores for Wilms tumor as well as other tumor types. Wilms tumor samples had significantly higher DNA repair scores than the other pediatric tumor types tested ($p = 0.0032$) (figure 2A) and the other adult kidney cancer types tested ($p < 0.0001$) (figure 2B). Additionally, there was a significant negative correlation between TIS and DNA repair scores within Wilms tumor samples ($r = -0.389$, $p < 0.0001$) (figure 2C). Wilms tumors also had significantly higher DNA repair scores than the matched normal kidney samples ($p < 0.0001$) (figure 2D), suggesting this was not merely a property of pediatric kidneys.

The significant negative association between DNA repair score and TIS in Wilms tumor led us to test whether the same observation could be detected in adult tumor types. Computing the correlation coefficient between DNA repair score and TIS across TCGA showed that most adult tumor types (24/31, 77%) displayed a negative association

between these two gene signatures (figure 3A). Since melanoma samples are relatively more accessible for further study, we looked more specifically within the TCGA metastatic melanoma samples and observed a significant negative correlation between TIS and both the 50-gene DNA repair score ($r = -0.235$, $p < 0.0001$) (figure 3B) and a score generated from all 480 genes in the MSigDB GO DNA Repair gene signature ($r = -0.397$, $p < 0.0001$) (figure 3C). This result suggested that adult melanoma displayed the same anti-correlation between DNA repair gene expression and TIS that was seen in Wilms tumor. Interestingly, this finding was not limited to tumor types that are generally immunotherapy-responsive, such as melanoma, and the strongest anti-correlation was actually observed in the poorly immunogenic glioblastoma multiforme tumor type.

It is well-established that loss of MSH2 and other DNA repair genes can rapidly promote the accumulation of mutations in cancer. However, the result of overexpression is not clear. We therefore examined whether high DNA repair gene expression was associated with a low TMB. In the TCGA melanoma samples, there was a mild association between DNA repair gene expression and total TMB ($r = 0.1416$, $p = 0.016$) (online supplemental file 3A). The negative association between DNA repair score and TIS in melanoma remained significant after correcting for effects of TMB ($r = -0.271$, $p < 0.0001$) (online supplemental file 3B). Furthermore, when mutation effects

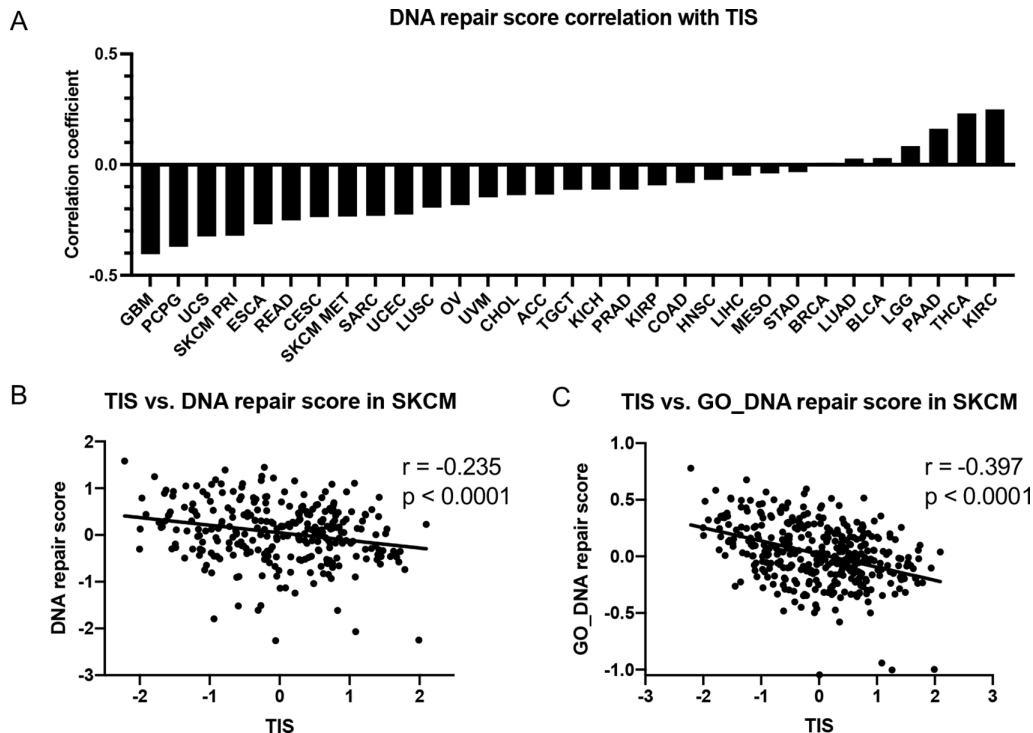


Figure 3 TIS significantly anti-correlates with DNA repair score in most TCGA tumor types, including melanoma. (A) Correlation coefficients for the correlation between TIS and DNA repair score in each TCGA tumor type. (B) Correlation between TIS and DNA repair score in TCGA metastatic melanoma samples. Pearson's correlation $r = -0.235$, $p < 0.0001$. (C) Correlation between TIS and GO_DNA repair gene score in TCGA metastatic melanoma samples. Pearson's correlation $r = -0.397$, $p < 0.0001$. TCGA, The Cancer Genome Atlas; TIS, tumor inflammation signature. SKCM: skin cancer, melanoma.

were regressed out of all adult tumors with mutation data, the majority of tumor types (25/29, 86%) retained a negative correlation between DNA repair score and TIS (online supplemental figure 3C). These results suggest that high expression of DNA repair pathway machinery restricts tumor immunogenicity by mechanisms other than preventing neoantigen accumulation. In contrast, there was a significant positive correlation in TCGA melanoma between TIS and a signature of type I interferon (IFN)-induced genes (*IFI44*, *LY6E*, *MX1*, *OAS3*) (online supplemental file 3d) and a signature of conventional dendritic cell type 1 (cDC1) genes (*BATF3*, *IRF8*, *THBD*, *CD1c*) (online supplemental figure 3E).¹⁵ This supports the notion that the presence of type I IFN signaling and cDC1 cells is associated with CD8⁺ T cell inflammation, and raises the possibility that high DNA repair gene expression may be interfering with that process at some level.

The relationship between DNA repair expression and T cell inflammation was examined more closely in melanoma tissue samples. *MSH2* was one of the top DNA repair genes identified from the Wilms tumor analysis and was confirmed to have a significant anti-correlation with TIS in melanoma (online supplemental figure 4). *MSH2* protein was therefore chosen as a DNA repair marker in these samples for validation, and there was a detectable range of both *MSH2*⁺ tumor cells and CD8⁺ T cells in melanoma samples (figure 4A). We performed immunofluorescence staining on pretreatment tumor

samples from a cohort of 26 patients with metastatic melanoma treated with anti-PD-1 therapy. Response was determined using RECIST V.1.1 criteria,¹⁶ and the cohort contained 21 responders (6 complete responders (CR), 7 partial responders (PR), and 8 with stable disease (SD)) as well as 5 non-responders (progressive disease (PD)). Tumor cells and CD8⁺ T cells were identified by the transcription factor *SOX10* and surface marker *CD8*, respectively. A significant negative correlation between CD8⁺ T cell numbers and *MSH2*⁺ *SOX10*⁺ tumor cell numbers was observed per ROI ($r = -0.255$) (figure 4B). In fact, there were no ROI quantified with both above-median numbers of *MSH2*⁺ *SOX10*⁺ tumor cells and above-median numbers of CD8⁺ T cells. Additionally, non-responders to anti-PD-1 therapy had significantly higher numbers of *MSH2*⁺ *SOX10*⁺ tumor cells than responders ($p < 0.0001$), whereas non-responders had significantly lower numbers of CD8⁺ T cells ($p = 0.0059$) (figure 4C). These results indicate that high *MSH2* expression is associated with diminished CD8⁺ T cell infiltration and lack of response to anti-PD-1 therapy.

DISCUSSION

Compared with adult tumor types, relatively little is known about the immune landscape of pediatric tumors and their associated mechanisms of immune resistance. Using RNA sequencing data, we showed that Wilms tumors demonstrate significantly lower TIS than matched

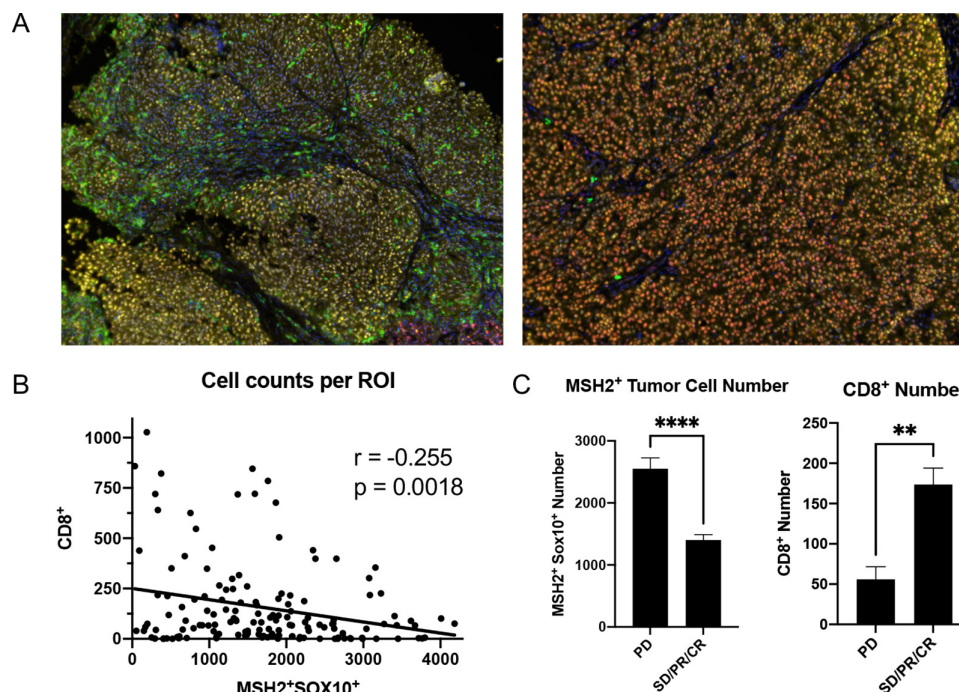


Figure 4 MSH2⁺ tumor cell numbers significantly anti-correlate with CD8⁺ T cells in patients with melanoma and are significantly higher in non-responders to anti-PD-1 immunotherapy. (A) Example images from immunofluorescence staining of melanoma tissues. MSH2 is shown in red, CD8 is green, SOX10 is yellow, and DAPI is blue. (B) Correlation of CD8⁺ cells and MSH2⁺SOX10⁺ in each 40× melanoma slide image, five images taken per sample. Pearson's correlation $r = -0.255$, $p = 0.0018$. (C) Quantification of MSH2⁺SOX10⁺ and CD8⁺ cells by ICB response category. Two-sided unpaired t-test. **, $p < 0.01$; ****, $p < 0.0001$. CR, complete responders; PD, progressive disease; PD-1, programmed cell death protein-1; PR, partial responders; ROI, regions of interest; SD, stable disease.

normal kidney samples, other pediatric tumor samples, and adult kidney tumor samples. Pathway analysis identified multiple types of DNA repair genes are upregulated in Wilms tumor and anti-correlated with TIS scores.

Surprisingly, we did not observe a strong association between DNA repair gene expression scores and total mutation numbers in melanoma, and the negative relationship between DNA repair score and TIS remained strong across TCGA when correcting for mutation count. This indicates a potential role for DNA repair genes outside of preventing the accumulation of somatic mutations and warrants further investigation. These data are consistent with our previously published results demonstrating lack of correlation between mutation load and immune gene signature among tumors in TCGA,¹⁵ arguing that cancer cell antigenicity and immunogenicity are independent events. It seems likely that upregulation of DNA repair pathways maintains cellular fitness, which in turn could lead to diminished immunogenicity. Rapidly proliferating cells experience high levels of replicative and oxidative stress that can lead to DNA damage.¹⁷ Disruption of specific DNA polymerases as well as repair enzymes such as BLM, BRCA2, and RNaseH2 promote genome instability and the formation of micronuclei, which can then be detected by the enzyme cGAS to trigger an innate immune response.^{18–22} For example, polymerase ζ -deficient cells accumulated micronuclei and induced expression of IFN-stimulated genes in a

cGAS- and STING-dependent manner.²³ In response to acute BRCA2 abrogation, tumor cells accumulated micronuclei and limited proliferation by G1 cell cycle arrest. As the cells adapted to chronic BRCA2 loss, they re-entered the cell cycle with a concomitant upregulation of IFN-stimulated genes that was dependent on STING and STAT1.²⁴ Additionally, the upregulation of IFN genes following loss of EXO1 or BLM could be reversed by knocking out TREX1, an enzyme that degrades cytosolic DNA.¹⁸ Taken together these data support the notion that DNA repair disruption can trigger innate immune activation through induction of IFN signaling following micronuclei sensing.

Our observations in Wilms tumor suggest the converse may also be true, and that increased tumor expression of DNA repair genes is associated with a less robust immune response, perhaps due to reduced cGAS-STING pathway activation. Previous work from our laboratory and others showed that type I IFN signaling is correlated with activated T cell gene signatures in human tumors and required for tumor-specific T-cell priming in mice.¹⁹ By creating a DNA repair score from the DNA repair genes identified in Wilms tumor, we were able to test whether DNA repair gene expression is negatively associated with T-cell inflammation in adult tumor types as well. It is known that high levels of tumor microsatellite instability are associated in adult tumors with increased lymphocyte infiltration, reduced metastasis, and improved survival

as well as response to checkpoint blockade immunotherapy.^{20 21}

Some tumors have been shown to upregulate DNA repair genes, such as *MGMT*, *RRM2*, *POLE2*, and *TTK*, which associated with increased invasiveness and metastasis, poor outcomes, and resistance to therapy.^{22 25–28} These observations led to the hypothesis that overexpression of MMR genes could improve cellular resistance to DNA lesions as well as survival following DNA damage.²⁹ In support of this hypothesis, overexpression of the base excision repair enzyme NTHL1 promoted oncogenic transformation of HBEC lung cells.³⁰ We believe high DNA repair gene expression could also promote tumor immune evasion, as we identified a significant negative correlation between DNA repair and activated T-cell signatures in the majority of TCGA tumor types. Additionally, we identified significantly higher numbers of cells positive for the DNA repair protein MSH2 in patients with melanoma with diminished CD8⁺ T-cell infiltration and lack of response to anti-PD-1 therapy.

While this work is limited by the correlative nature of examining human tissues, future studies will be required to develop novel mouse models to investigate a causative relationship between high DNA repair gene expression and tumor immune evasion. The large collection of DNA repair genes we observed to be coordinately overexpressed suggests that the phenotype is unlikely to be explained by mutations in a single gene. Rather, it is likely that a more complex mechanism affecting multiple DNA repair genes through shared transcription factors or epigenetic modifications drives their coordinated upregulation. DNA repair pathways are known to be regulated in a complex network, as impairment in one pathway can lead to dependence on others and deleterious mutations in multiple pathways leads to higher immune gene expression in tumors.²¹ In the future, DNA repair pathway inhibitors may be worth pursuing as a potential strategy to improve host immune system activation. This notion is supported by the observation that PARP inhibitors can improve immunotherapy efficacy in vivo, in part by promoting STING pathway activation in host immune cells.^{31 32}

Twitter Riyue Bao @RiyueSunnyBao

Acknowledgements We would like to thank the University of Chicago Human Immune Monitoring Core, specifically Yuanyuan Zha, for biobanking melanoma tissue and immunofluorescence support. We would also like to acknowledge Terri Li and the University of Chicago Human Tissue Resources Center for assistance with processing tissue samples.

Contributors EFH, RB, and TFG designed the RNA sequencing study. KH did the immunofluorescence staining and imaging. EFH and RB performed the data analysis. EFH and TFG wrote the paper. All authors reviewed and approved the paper.

Funding This work was supported by R35CA210098 from the NCI. EFH is supported by NIH F30CA250255. KH is supported by Japan Cancer Society Relay for Life Award (2017), Japan Society for the Promotion of Science Overseas Research Fellowship (2019–2020).

Competing interests None declared.

Patient consent for publication Not applicable.

Ethics approval Not applicable.

Provenance and peer review Not commissioned; externally peer reviewed.

Data availability statement Data are available in a public, open access repository. All data relevant to the study are included in the article or uploaded as supplementary information.

Supplemental material This content has been supplied by the author(s). It has not been vetted by BMJ Publishing Group Limited (BMJ) and may not have been peer-reviewed. Any opinions or recommendations discussed are solely those of the author(s) and are not endorsed by BMJ. BMJ disclaims all liability and responsibility arising from any reliance placed on the content. Where the content includes any translated material, BMJ does not warrant the accuracy and reliability of the translations (including but not limited to local regulations, clinical guidelines, terminology, drug names and drug dosages), and is not responsible for any error and/or omissions arising from translation and adaptation or otherwise.

Open access This is an open access article distributed in accordance with the Creative Commons Attribution Non Commercial (CC BY-NC 4.0) license, which permits others to distribute, remix, adapt, build upon this work non-commercially, and license their derivative works on different terms, provided the original work is properly cited, appropriate credit is given, any changes made indicated, and the use is non-commercial. See <http://creativecommons.org/licenses/by-nc/4.0/>.

ORCID iDs

Emily F Higgs <http://orcid.org/0000-0003-2477-8549>

Riyue Bao <http://orcid.org/0000-0002-6105-1704>

REFERENCES

- 1 Szychot E, Apps J, Pritchard-Jones K. Wilms' tumour: biology, diagnosis and treatment. *Translational Pediatrics* 2014;3:124.
- 2 Stahl D, Knoll R, Gentles AJ, *et al*. Prognostic gene expression, stemness and immune microenvironment in pediatric tumors. *Cancers* 2021;13:854.
- 3 Schmitt J, Keller A, Nourkami-Tutdibi N, *et al*. Autoantibody signature differentiates Wilms tumor patients from neuroblastoma patients. *PLoS One* 2011;6:e28951.
- 4 Danaher P, Warren S, Dennis L, *et al*. Gene expression markers of tumor infiltrating leukocytes. *J Immunother Cancer* 2017;5:18.
- 5 Motzer RJ, Escudier B, McDermott DF, *et al*. Nivolumab versus everolimus in advanced renal-cell carcinoma. *N Engl J Med* 2015;373:1803–13.
- 6 Albiges L, Pouessel D, Beylot-Barry M, *et al*. Nivolumab in metastatic nonclear cell renal cell carcinoma: first results of the AcSe prospective study. *JCO* 2020;38:699.
- 7 Li C-M, Kim CE, Margolin AA, *et al*. Ctnnb1 mutations and overexpression of Wnt/beta-catenin target genes in WT1-mutant Wilms' tumors. *Am J Pathol* 2004;165:1943–53.
- 8 Spranger S, Bao R, Gajewski TF. Melanoma-intrinsic β -catenin signalling prevents anti-tumour immunity. *Nature* 2015;523:231–5.
- 9 Luke JJ, Bao R, Sweis RF, *et al*. WNT/ β -catenin pathway activation correlates with immune exclusion across human cancers. *Clin Cancer Res clincanres* 2019;1942.2018.
- 10 Holl EK, Routh JC, Johnston AV, *et al*. Immune expression in children with Wilms tumor: a pilot study. *J Pediatr Urol* 2019;15:441.e1–441.e8.
- 11 Routh JC, Ashley RA, Sebo TJ, *et al*. B7-H1 expression in Wilms tumor: correlation with tumor biology and disease recurrence. *J Urol* 2008;179:1954–60.
- 12 Mardanpour K, Rahbar M, Mardanpour S, *et al*. CD8+ T-cell lymphocytes infiltration predict clinical outcomes in Wilms' tumor. *Tumour Biol* 2020;42:101042832097597.
- 13 Young MD, Mitchell TJ, Vieira Braga FA, *et al*. Single-cell transcriptomes from human kidneys reveal the cellular identity of renal tumors. *Science* 2018;361:594–9.
- 14 Danaher P, Warren S, Lu R, *et al*. Pan-cancer adaptive immune resistance as defined by the tumor inflammation signature (TIS): results from the cancer genome atlas (TCGA). *J Immunother Cancer* 2018;6:63.
- 15 Spranger S, Luke JJ, Bao R, *et al*. Density of immunogenic antigens does not explain the presence or absence of the T-cell-inflamed tumor microenvironment in melanoma. *Proc Natl Acad Sci U S A* 2016;113:E7759–68.
- 16 Eisenhauer EA, Therasse P, Bogaerts J, *et al*. New response evaluation criteria in solid tumours: revised RECIST guideline (version 1.1). *Eur J Cancer* 2009;45:228–47.

- 17 Gaillard H, García-Muse T, Aguilera A. Replication stress and cancer. *Nat Rev Cancer* 2015;15:276–89.
- 18 Erdal E, Haider S, Rehwinkel J, et al. A prosurvival DNA damage-induced cytoplasmic interferon response is mediated by end resection factors and is limited by TREX1. *Genes Dev* 2017;31:353–69.
- 19 Fuertes MB, Woo S-R, Burnett B, et al. Type I interferon response and innate immune sensing of cancer. *Trends Immunol* 2013;34:67–73.
- 20 Sarasin A, Kauffmann A. Overexpression of DNA repair genes is associated with metastasis: a new hypothesis. *Mutat Res Rev Mutat Res* 2008;659:49–55.
- 21 Wang Z, Zhao J, Wang G, et al. Comutations in DNA damage response pathways serve as potential biomarkers for immune checkpoint blockade. *Cancer Res* 2018;78:6486–96.
- 22 Sharma S et al. Role of MGMT in tumor development, progression, diagnosis, treatment and prognosis. *Anticancer research* 2009;10.
- 23 Martin SK, Tomida J, Wood RD. Disruption of DNA polymerase ζ engages an innate immune response. *Cell Rep* 2021;34:108775.
- 24 Reisländer T, Lombardi EP, Groelly FJ, et al. BRCA2 abrogation triggers innate immune responses potentiated by treatment with PARP inhibitors. *Nat Commun* 2019;10:3143.
- 25 Mazzu YZ, Armenia J, Chakraborty G, et al. A novel mechanism driving poor-prognosis prostate cancer: overexpression of the DNA repair gene, ribonucleotide reductase small subunit M2 (RRM2). *Clin Cancer Res* 2019;25:4480–92.
- 26 Wu Z, Wang Y-M, Dai Y, et al. POLE2 serves as a prognostic biomarker and is associated with immune infiltration in squamous cell lung cancer. *Med Sci Monit* 2020;26:e921430.
- 27 Guo E, Wu C, Ming J, et al. The clinical significance of DNA damage repair signatures in clear cell renal cell carcinoma. *Front Genet* 2020;11:593039.
- 28 Mathews LA, Cabarcas SM, Hurt EM, et al. Increased expression of DNA repair genes in invasive human pancreatic cancer cells. *Pancreas* 2011;40:730–9.
- 29 Kauffmann A, Rosselli F, Lazar V, et al. High expression of DNA repair pathways is associated with metastasis in melanoma patients. *Oncogene* 2008;27:565–73.
- 30 Limpose KL, Trego KS, Li Z, et al. Overexpression of the base excision repair NTHL1 glycosylase causes genomic instability and early cellular hallmarks of cancer. *Nucleic Acids Res* 2018;46:4515–32.
- 31 Gupta P Det al. PARP and PI3K inhibitor combination therapy eradicates c-MYC-driven murine prostate cancers via cGAS/STING pathway activation within tumor-associated macrophages. *bioRxiv* 2020:2020.07.17.198598.
- 32 Ding L, Kim H-J, Wang Q, et al. Parp inhibition elicits STING-dependent antitumor immunity in BRCA1-deficient ovarian cancer. *Cell Rep* 2018;25:2972–80.